

# A Study of $(\alpha, p)$ Reactions along the $\alpha p$ -Process Path and their Influence on Type 1 X-ray Burst Light Curves

The  $^{30}\text{S}(\alpha, p)$  and  $^{34}\text{Ar}(\alpha, p)$  reactions have both been identified in several Type-1 X-ray Bursts (XRBs) sensitivity studies as significant influential reactions within the  $\alpha p$ -process. According to 1-D XRB models, the strength of these two reactions can affect not only final abundance patterns XRB ashes, but also possibly the bolometric shapes of double-peaked XRB light curves. Given the lifetimes of the nuclei involved, very little experimental information exists for these two reactions, therefore, XRB models depend on a statistical Hauser-Feshbach (HF) model to predict the reaction rate. Recently, questions on the reliability of HF predicted rates for these reactions arise due to level density considerations in the compound nuclei ( $^{34}\text{Ar}$  and  $^{38}\text{Ca}$ ).

With this in mind, we have performed high energy-resolution forward-angle  $^{36}\text{Ar}(p, t)^{34}\text{Ar}$  and  $^{40}\text{Ca}(p, t)^{38}\text{Ca}$  measurements at RCNP and iThemba LABS, respectively, in order to identify levels in  $^{34}\text{Ar}$  and  $^{38}\text{Ca}$  that would possibly act as  $(\alpha, p)$  resonances in their respective reactions. Both experiments utilized magnetic spectrographs with dispersion matched beamlines, thus achieving the needed high energy resolution to resolve possible closely spaced states. The results from these works are illustrated in Fig. 1.

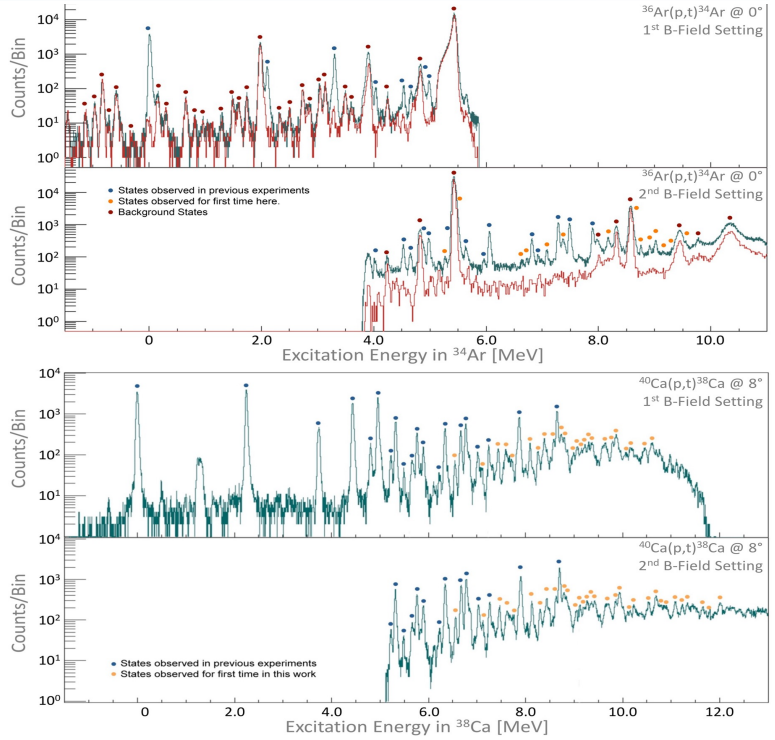


Figure 1: Final focal plane spectra showing states in  $^{34}\text{Ar}$  (top) and  $^{38}\text{Ca}$  (bottom) for the two experiments performed at RCNP and iThemba, respectively. All states identified for the first time in these works are illustrated with orange dots.

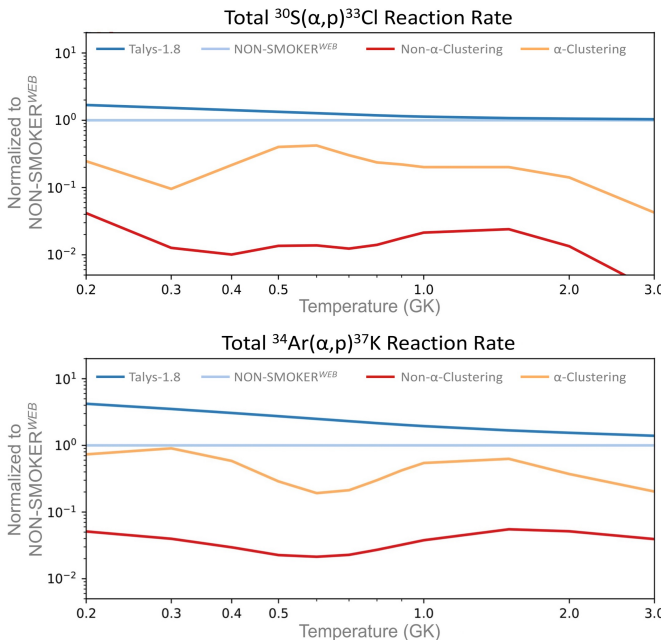


Figure 2: Comparisons of the  $^{30}\text{S}(\alpha, p)$  and  $^{34}\text{Ar}(\alpha, p)$  reaction rates as derived based on the states observed in these works (Median Rates 1 & 2), along with two HF model predicted rates (Talys-1.8 and JINA REACLIB)

With precise energy information of levels in  $^{34}\text{Ar}$  and  $^{38}\text{Ca}$  that can possibly act as resonances in the  $^{30}\text{S}(\alpha, p)$  and  $^{34}\text{Ar}(\alpha, p)$  reaction, total reaction rates were calculated based on a narrow resonance formalism. Additionally, models were used to fill in missing spin and spectroscopic information. For spins, states were assigned values based on randomly sampling Back-Shifted Fermi-Gas model spin distributions, while for  $\alpha$ -spectroscopic information, two approaches were utilized (one representing  $\alpha$ -clustering and the other representing non- $\alpha$ -clustering).  $\alpha$ -Spectroscopic factors in the case of  $\alpha$ -clustering were derived using shell model calculations, while in the case of non- $\alpha$ -clustering a flat global value was taken.

The total reaction rates of  $^{30}\text{S}(\alpha, p)$  and  $^{34}\text{Ar}(\alpha, p)$ , as derived in these works, are compared to two HF model predicted rates in Fig. 2. In both cases, the non- $\alpha$ -cluster rate is significantly lower than HF predicted rates, suggesting that that level densities in  $^{34}\text{Ar}$  and  $^{38}\text{Ca}$  (based on levels observed here) are not high enough to support the statistical approach of HF models. Furthermore, comparing the  $\alpha$ -cluster rate to the non- $\alpha$ -cluster rate, illustrates the possibility of one or two strong  $\alpha$ -cluster states dominating the rate within a given temperature range.